

**Electronic Supporting Information (ESI) concerning the manuscript:**

**Photo- and thermo-induced spin crossover in a cyanide-bridged {Mo<sup>V</sup><sub>2</sub>Fe<sup>II</sup><sub>2</sub>} rhombus molecule**

Abhishake Mondal, Yanling Li, Lise-Marie Chamoreau, Mannan Seuleiman, Lionel Rechignat, Azzedine Bousseksou, Marie-Laure Boillot and Rodrigue Lescouëzec

## Experimental section

- Syntheses
- Crystal structure data collection and refinement
- Magnetic measurements
- Spectroscopic measurements (FT-IR, UV-vis and Mössbauer spectroscopies)

**Figure S1.** Perspective view of the  $\{\text{Mo}^{\text{V}}_2\text{Fe}^{\text{II}}_2\}$  rhombus unit in **1** together with atom labelling for the iron and molybdenum coordination spheres (grey, blue, red orange and yellow spheres are carbon, nitrogen, oxygen, iron, and molybdenum atoms; hydrogen atoms are omitted for clarity).

**Figure S2.** Perspective view of the rhombus core in **1** (a) and of the  $\{\text{Mo}(\text{CN})_8\}$  coordination sphere as calculated through the SHAPE program (b and c).<sup>[S2]</sup> The main axes of the square antiprism coordination sphere of Mo1 and Mo2 are almost orthogonal (grey, blue, red orange and yellow spheres are carbon, nitrogen, oxygen, iron, and molybdenum atoms; hydrogen atoms are omitted for clarity).

**Figure S3.** Thermo-gravimetric analysis of **1** in the 20-400 °C range at 1 K/min (under a nitrogen flow).

**Figure S4.** Plots of the  $\chi_M T$  vs.  $T$  of **1** for fresh (black) and previously dehydrated samples: dehydration at 353 K (blue) and 400 K (red).

**Figure S5.** Variable temperature FT-IR spectra of **1** in the 400-4000 (top) and 1950-2200  $\text{cm}^{-1}$  ranges.

**Figure S6.** Solid-state UV-vis absorption spectra of **1** at different temperatures (sample dispersed in a KBr pellet).

**Figure S7.** Plots of  $\chi_M T$  versus irradiation time for a dehydrated sample of **1** at 405, 532, 635 and 808 nm at a laser power of 5, 10, 12 and 6  $\text{mW}/\text{cm}^2$ , respectively (the jump observed on the right side of the curves occur as the lights are switched off and they are ascribed to the heating effect of the laser lights).

**Tables S1.** Estimates of the relative amounts of high-spin Fe<sup>II</sup> ions in **1** obtained from Mössbauer spectroscopy and magnetic susceptibility measurements.

## Experimental Section and Physical Techniques

**Syntheses.** The bik ligand and the  $[N(C_4H_9)_4]_3[Mo^V(CN)_8]$  complex were prepared as previously described.<sup>S1</sup> The  $[Fe(bik)_2(S)_2](BF_4)_2$  complex was prepared *in situ* in acetonitrile (15 mL) reacting stoichiometric amounts of  $Fe(BF_4)_2 \cdot 6H_2O$  (34.1 mg, 0.1 mmol) and bik (38 mg, 0.2 mmol). Acetonitrile solutions of  $[N(C_4H_9)_4]_3[Mo^V(CN)_8]$  (107.6 mg, 0.1 mmol in 10 mL) and  $H^{MeIm}Cl$  (35.5 mg, 0.3 mmol, in 5 mL) were added dropwise to that containing  $[Fe(bik)_2(S)_2](BF_4)_2$  ( $H^{MeIm}Cl$  is the 1-methylimidazolium chloride salt). The resulting purple-red solution was stirred at room temperature for 30 min and then filtered. Light red plate-like crystals of  $\{[Mo(CN)_8]_2[Fe(bik)_2]_2\}(H^{MeIm})_2 \cdot 6H_2O \cdot CH_3CN$  ( $H^{MeIm}$  : 1-methylimidazole) were obtained in a good yield (ca. 75%) by slow evaporation of the solution in a few days. Elemental analyses match with partially dehydrated sample of formula: **1**:  $5H_2O \cdot CH_3CN$   $C_{62}H_{67}Fe_2Mo_2N_{37}O_9$  (1778.10 g/mol). Elemental Analysis cacl (%): C: 41.86; H: 3.80; N: 29.15; found (%): C: 41.54; H: 3.53; N: 27.80.

[S1] (a) N. Braussaud, T. Ruther, K. J. Cavell, B. W. Sketon, A. H. White, *Synthesis*, **2001**, 626; (b) F. Bonadio et al. *Inorg. Synthesis*, **2004**, vol 34, 156 (Eds: J.R. Shapley) WILEY-VCH.

**Elemental Analysis** (C, H, N) were carried out at the SIARE service of the Université Pierre et Marie Curie, Paris6.

**Thermogravimetric analysis** has been carried out on a TAI instrument SDT Q600 under 1 bar nitrogen atmosphere.

**Crystal data** for **1**:  $C_{62}H_{67}Fe_2Mo_2N_{37}O_9$ , Mw = 1778.1 g.mol<sup>-1</sup>, monoclinic,  $P 2_1/m$ ,  $a = 13.0803(4)$ ,  $b = 17.4938(6)$ ,  $c = 17.6157(5)$  Å,  $\beta = 95.160(2)$  °,  $V = 4014.6(2)$  Å<sup>3</sup>,  $Z = 2$ ,  $T = 200(2)$  K,  $\mu = 0.735$  mm<sup>-1</sup>, 43140 reflections measured, 9462 independent ( $R_{int} = 0.0446$ ), 6593 observed [ $I \geq 2\sigma(I)$ ], 517 parameters, final R indices  $R_1$  [ $I \geq 2\sigma(I)$ ] = 0.0516 and  $wR_2$  (all data) = 0.1587, GOF on  $F^2$  = 1.027, max/min residual electron density = 1.19/-0.83 e.Å<sup>-3</sup>. A single crystal (dark red square plate-like) of **1** was mounted onto a Hampton cryoloop, and transferred in a cold nitrogen gas stream. Intensity data were collected with a BRUKER Kappa-APEXII diffractometer with graphite-monochromated Mo-Kα radiation ( $\lambda = 0.71073$  Å). Data collection was performed with APEX2 suite.\* Unit-cell parameters refinement, integration and data reduction were carried out with SAINT program.\* SADABS\* was used for scaling and multi-scan absorption corrections. In the WinGX suite of programs (L. J. Farrugia, *J. Appl. Crystallogr.*, 1999, **32**, 837-838), the structure was solved with Sir97 (A. Altomare, M. C. Burla, M. Camalli, G. L. Cascarano, C. Giacovazzo, A. Guagliardi, A. G. G. Moliterni, G. Polidori and R. Spagna, *J. Appl. Crystallogr.*, 1999, **32**, 115-119) program and refined by full-matrix least-squares methods using SHELXL-97 (G. M. Sheldrick, *Acta Crystallogr.*, A64, 2008, 112-122).

All non-hydrogen atoms of the anion were refined anisotropically while the atoms of cations and most water molecules were refined isotropically. A model of disorder was introduced for both ( $H^{MeIm}$ ) cations. Hydrogen atoms were placed at calculated positions. In both structures, the anion undergoes a few geometrical restraints.

CCDC 970795, contain the supplementary crystallographic data for this paper. These data can be obtained free of charge from The Cambridge Crystallographic Data Centre via [www.ccdc.cam.ac.uk/data\\_request/cif](http://www.ccdc.cam.ac.uk/data_request/cif).

\*Bruker AXS Bruker AXS Inc., Madison, Wisconsin, USA.

**Variable-temperature (2.0-400 K) magnetic measurements** were carried out with a MPMS-XL Quantum Design SQUID magnetometer under a 2500 Oe applied magnetic field and using a scan rate of 2K/min. In a typical experiment, the sample packed in a polyethylene bag was introduced in the SQUID at 200 K under helium flow and frozen before purging under vacuum. The susceptibility measurements were first carried out from 200 to 2 K, then from 2 K to 400 K, and finally from 400 to 2 K. The fresh sample was filtered from the mother solution just before the SQUID experiment and the dehydrated samples were measured just after heating the sample in the TGA machine up to 353 and 400 K (at 2 K/min under N<sub>2</sub> flow).

**Variable-temperature FT-IR spectra** were carried out on a Perkin Elmer spectrometer (Spectrum 100) equipped with the eurolabo variable-temperature cell (21525) and Specac temperature controller (20120). The measurements were performed on KBr pellets (approximately 1 mg of fresh crystallites of **1** were dispersed without grinding with *ca.* 100 mg of KBr that was previously ground) in the 400-4000 cm<sup>-1</sup> range between 100 and 400 K.

**Variable-temperature solid-state UV-vis spectra** were measured in the range 350-2500 nm on a CARY 5000 double-beam spectrophotometer equipped with an APD Cryogenic closed-cycle helium system including a DMX-1E cryostat and a DE-202 expander. The sample was prepared in a similar way as for the FT-IR study: approximately 1 mg of fresh crystallites of **1** were dispersed without any grinding in *ca.* 100 mg of KBr, this later being previously ground.

**Mössbauer Spectroscopy.** <sup>57</sup>Fe Mössbauer spectra have been recorded using a conventional constant-acceleration-type spectrometer equipped with a 50 mCi <sup>57</sup>Co source and a flow-type, liquid-helium cryostat. Spectra of the samples (*ca.* 50 mg) were recorded at 300 and 80 K under reduced helium pressure. The fresh sample has been measured just after filtration from the mother solution whereas the dehydrated phase has been measured after heating the sample up to 400 K. Least-squares fittings of the Mössbauer spectra have been carried out with the assumption of Lorentzian line shapes using Recoil software package.

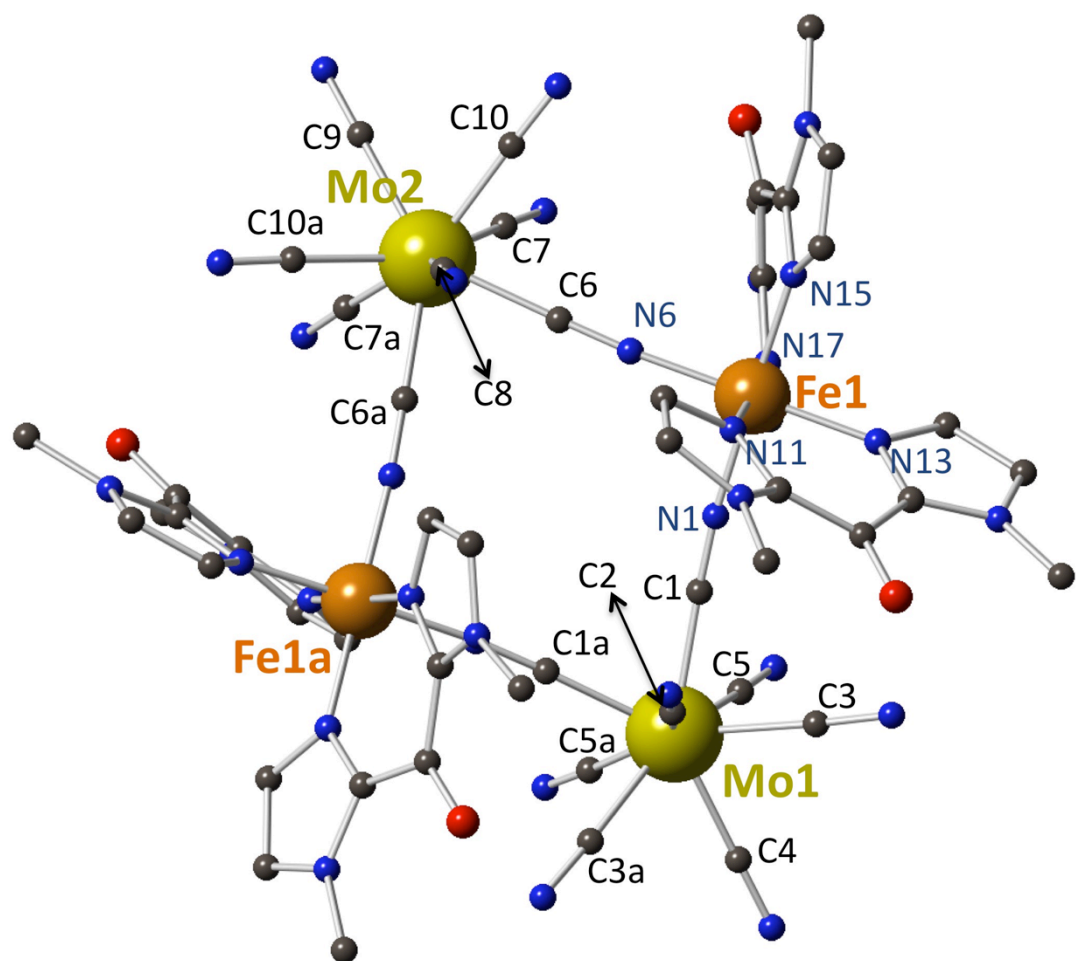


**Figure S1.** Perspective view of the  $\{Mo^V_2Fe^{II}_2\}$  rhombus unit in **1** together with atom labelling for the iron and molybdenum coordination spheres (grey, blue, red orange and yellow spheres are carbon, nitrogen, oxygen, iron, and molybdenum atoms; hydrogen atoms are omitted for clarity).

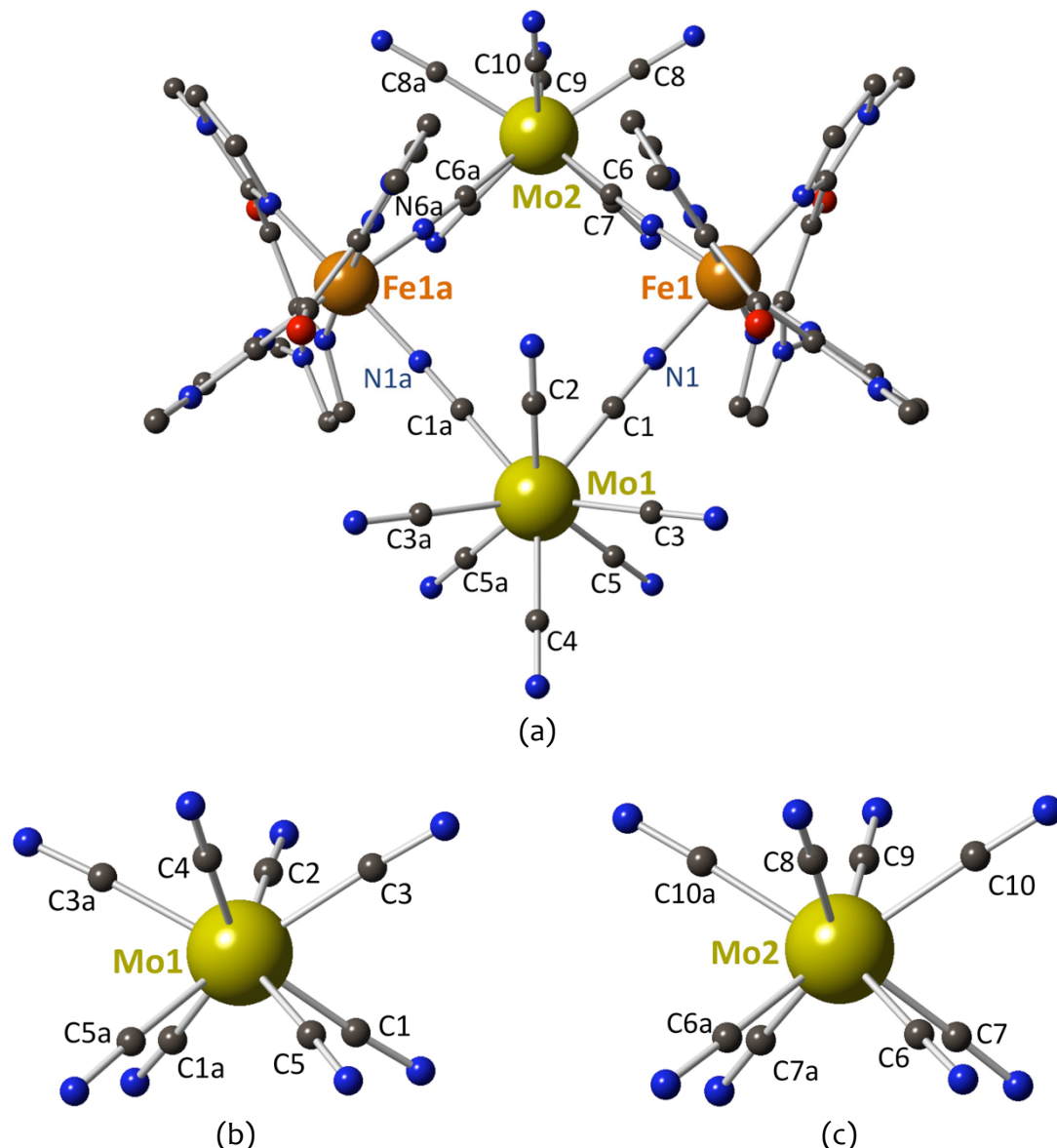


**Figure S2.** Perspective view of the rhombus core in **1** (a) and of the  $\{\text{Mo}(\text{CN})_8\}$  coordination sphere as calculated through the SHAPE program (b and c).<sup>[S2]</sup> The main axes of the square antiprism coordination sphere of Mo1 and Mo2 are almost orthogonal (grey, blue, red, orange and yellow spheres are carbon, nitrogen, oxygen, iron, and molybdenum atoms; hydrogen atoms are omitted for clarity).

In order to determine the geometry around the Mo atoms, we performed a continuous shape measure (CShM) analysis.<sup>[S2]</sup> The reported values allow to evaluate the match between an idealized polyhedron and the actual coordination sphere: the lower the value is and the closer the actual coordination sphere is to the ideal polyhedron. The thirteen polyhedrons reported for octacoordinated complexes have been probed following the approach described by D. Casanova *et al.*<sup>[S1b]</sup> For the two molybdenum atoms, the lowest value calculated by SHAPE is obtained for the square antiprism, the two lowest values being close to each other, 0.147 and 0.113 for Mo1 and Mo2, respectively.

[S2] (a) M. Llunell, D. Casanova, J. Cirera, J. M. Bifill, P. Alemany, S. Alvarez, M. Pinsky, D. Avnir, SHAPE, v2, Barcelona, 2005; (b) D. Casanova, M. Llunell, P. Alemany, S. Alvarez, Chem. Eur. J., **2005**, 11, 1479.

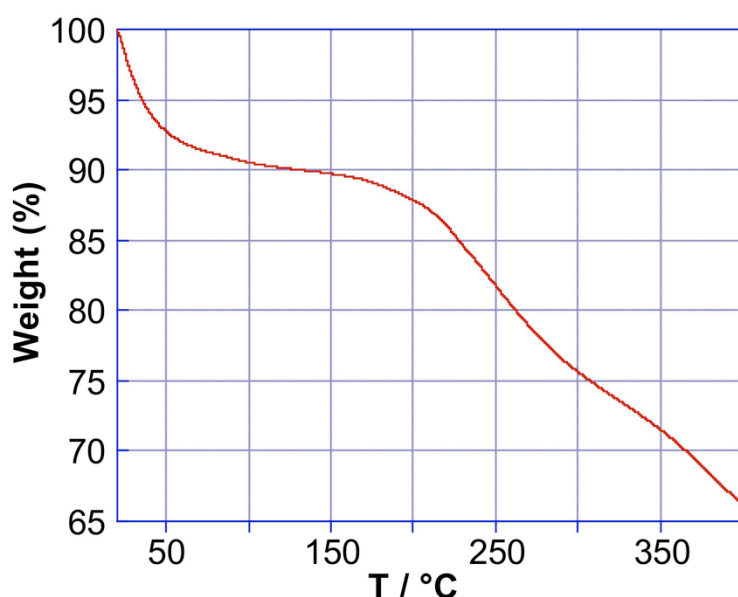


**Figure S3.** Thermo-gravimetric analysis of **1** in the 20–400 °C range at 1 K/min (under a nitrogen flow).

Compound **1** has been studied by thermogravimetric analysis (TGA) under a N<sub>2</sub> flow. It exhibits a significant weight loss from room temperature up to 120 °C, which corresponds to about 10 % of the total sample mass. At higher temperatures, the compound is stable under nitrogen atmosphere up to approximately 170 °C. The important weight loss observed at room temperature is consistent with the rapid loss of crystallinity of **1** as the sample is removed from the mother liquor. It corresponds to the removal of the crystallization solvent molecules (8.3%) observed by single-crystal XRD (six water and one acetonitrile molecules would correspond to 8.3 % of the sample weight) and very likely, solid wetting.

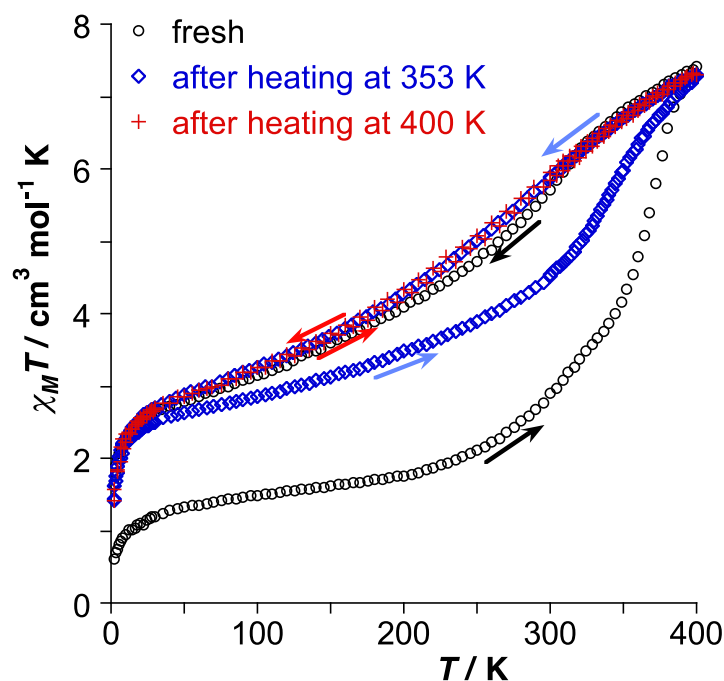


**Figure S4.** Plots of the  $\chi_M T$  vs.  $T$  of **1** for fresh (black) and previously dehydrated samples\*: dehydration at 353 K (blue) and 400 K (red).

The samples were introduced in the SQUID at 200 K. In all cases, the  $\chi_M T$  product was first measured upon cooling from 200 to 2 K, and upon heating from 2 to 400 K (the points obtained upon cooling and heating in the 2–200 K range overlap at that stage). Then the  $\chi_M T$  product was measured from 400 to 2 K. All these measurements have been performed out at two 2 K/min.

\*The dehydrated samples were obtained by heating the samples in the TGA machine up to 353 or 400 K (2 K/min under  $\text{N}_2$  flow) and the fresh sample was filtered from the mother solution, and packed in a polyethylene bag just before the SQUID experiment.

These measurements show a clear dependence of the  $\chi_M T$  value on the hydration grade. However, after full dehydration in the SQUID and/or by heating in TGA instrument, all the curves merge with the red one, which shows a smooth and partial spin transition.

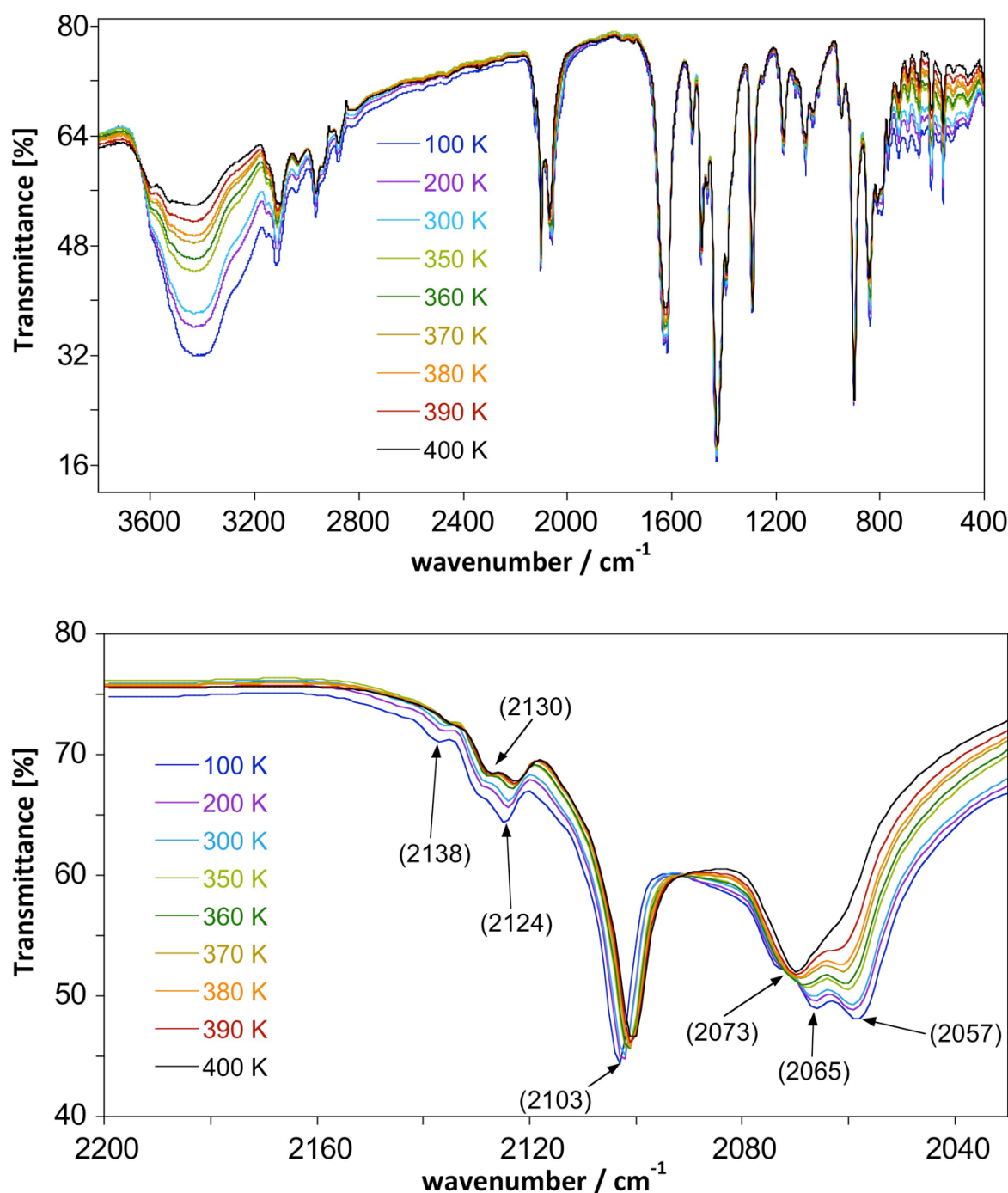


**Figure S5.** Variable temperature FT-IR spectra of **1** in the 400-4000 (top) and 1950-2200 (bottom) cm<sup>-1</sup> ranges.

The FT-IR spectrum of **1** does not significantly evolve in the 100 - 400 K temperature range, except for the broad band located near 3400 cm<sup>-1</sup> and ascribed to the O-H stretching vibrations of the water crystallization molecules. Overall, all other vibrations increase by 2-3 cm<sup>-1</sup> and become better resolved upon cooling. Slight shifts are also observed in the cyanide stretching frequencies. The most striking change in this energy range is the intensity decrease of the peaks at 2057 and 2065 cm<sup>-1</sup>.

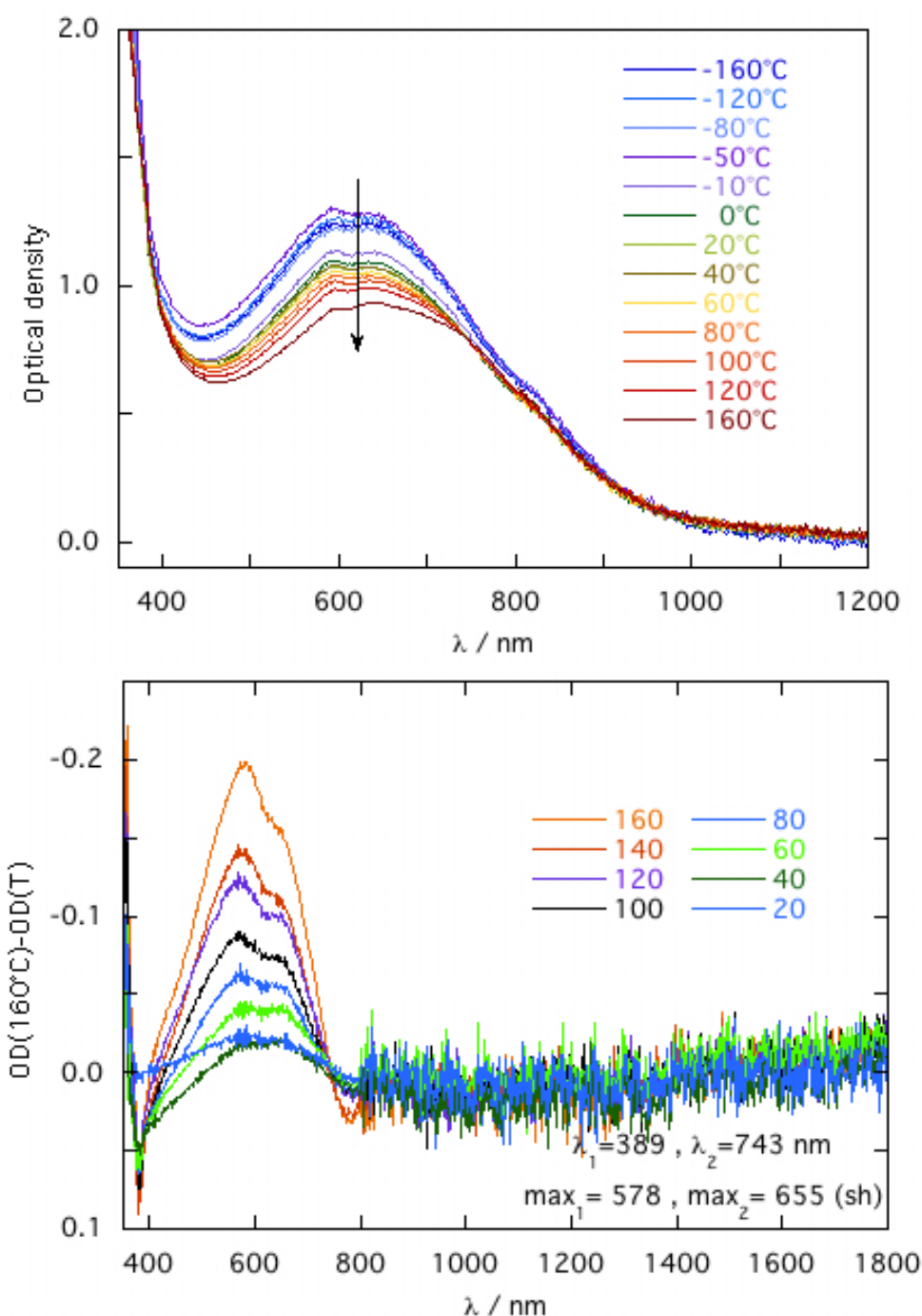


**Figure S6.** Top: solid-state UV-vis absorption spectra of **1** in the -160 – 160 °C temperature range (sample dispersed in a KBr pellet); Bottom: difference spectra  $\text{OD}(160^\circ\text{C}) - \text{OD}(T)$ . Isosbestic points are observed at  $\lambda_1 = 389$  and  $\lambda_2 = 743$  nm, and maxima at ca. 590 and 740 nm.

The solid-state UV-vis measurements of **1** exhibits a broad band centred near 620 nm, which can be ascribed to the metal-to-ligand charge transfer (MLCT) band of the  $[\text{Fe}^{\text{II}}(\text{bik})_2(\text{NC})_2]$  chromophores (see reference 7 by A. Mondal et al, *Chem. Commun.* 2012, **48**, 5653). The intensity decrease of this band upon heating is in agreement with the electronic rearrangement occurring in this chromophore.

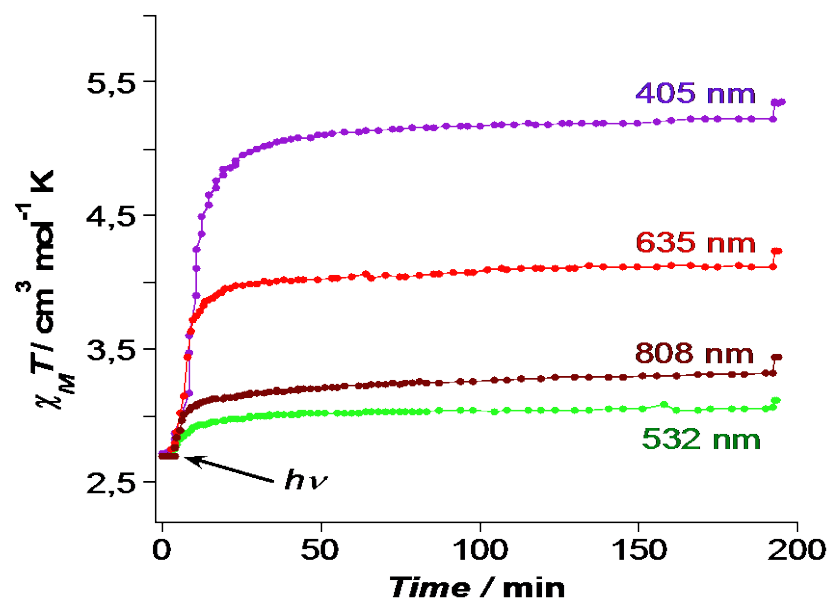


**Figure S8.** Plots of  $\chi_M T$  versus irradiation time for a dehydrated sample of **1** at 405, 532, 635 and 808 nm at a laser power of 5, 10, 12 and 6 mW/cm<sup>2</sup>, respectively (the jump observed on the right hand side of the curves occur as the lights are switched off and they are ascribed to the heating effect of the laser lights).

The  $\chi_M T$  values obtained after the irradiation with the 635, 808 and 532 nm laser lights are 3.93, 3.12 and 2.83 cm<sup>3</sup> mol<sup>-1</sup> K, respectively.

	Instrument	80 K	300 K
Fresh sample	Mössbauer spectroscopy	7 %	32 %
Fresh sample, before heating in the SQUID under reduced pressure at 400 K	SQUID magnetometer	9 % ( $1.42 - 0.75 = 0.629 \text{ cm}^3 \text{ mol}^{-1} \text{ K}$ )	29 % ( $2.83 - 0.75 = 2.08 \text{ cm}^3 \text{ mol}^{-1} \text{ K}$ )
After heating up to 400 K in the spectrometer	Mössbauer spectroscopy	24 %	45 %
dehydrated sample (TGA up to 353 K), before heating in the SQUID under reduced pressure at 400 K	SQUID magnetometer	27 % ( $2.76 - 0.75 = 2.01 \text{ cm}^3 \text{ mol}^{-1} \text{ K}$ )	51 % ( $4.49 - 0.75 = 3.74 \text{ cm}^3 \text{ mol}^{-1} \text{ K}$ )
Fresh sample, after heating in the SQUID under reduced pressure at 400 K	SQUID magnetometer	31 % ( $3.0 - 0.75 = 2.25 \text{ cm}^3 \text{ mol}^{-1} \text{ K}$ )	68 % ( $5.71 - 0.75 = 4.96 \text{ cm}^3 \text{ mol}^{-1} \text{ K}$ )
dehydrated sample (TGA up to 353 K), after heating in the SQUID under reduced pressure at 400 K	SQUID magnetometer	32 % ( $3.10 - 0.75 = 2.35 \text{ cm}^3 \text{ mol}^{-1} \text{ K}$ )	70 % ( $5.85 - 0.75 = 5.10 \text{ cm}^3 \text{ mol}^{-1} \text{ K}$ )
dehydrated sample (TGA up to 400 K)	SQUID magnetometer	32 % ( $3.10 - 0.75 = 2.35 \text{ cm}^3 \text{ mol}^{-1} \text{ K}$ )	70 % ( $5.87 - 0.75 = 5.12 \text{ cm}^3 \text{ mol}^{-1} \text{ K}$ )

**Table S1.** Estimates of the relative amounts of high-spin Fe<sup>II</sup> ions in **1** obtained from Mössbauer spectroscopy and magnetic susceptibility measurements.

The estimates derived from the magnetometry measurements were obtained by assuming  $\chi_M T$  values of 3.63 ( $g = 2.2$ ) and 0.375 ( $g = 2$ )  $\text{cm}^3 \text{ mol}^{-1} \text{ K}$  for the HS Fe<sup>II</sup> and Mo<sup>V</sup> ions, respectively. The contribution of the two paramagnetic Mo<sup>V</sup> ions was therefore removed by subtracting 0.75  $\text{cm}^3 \text{ mol}^{-1} \text{ K}$  to the experimental  $\chi_M T$  values. These estimates are more reliable at 300 K than at 80 K as magnetic exchange interaction between the Fe<sup>II</sup> and Mo<sup>V</sup> paramagnetic ions can affect the measured  $\chi_M T$  value.

The relative amounts of high-spin Fe<sup>II</sup> ions obtained from Mössbauer spectroscopy and magnetometry agree well for the fresh samples (ca. 8 and 30 % at 80 and 300 K, respectively). The discrepancies observed for the dehydrated samples are likely due to the different experimental conditions, which could lead to different hydration grades. Indeed, the magnetometry measurements showed that the  $\chi_M T$  value is very much dependent on the dehydration rate (Fig. S4), and the amount of HS Fe<sup>II</sup> tends to increase as the compound loses its crystallization solvent molecules.